energies

MDPI

Article

Estimating the State of Charge of Lithium-Ion Batteries Based on the Transfer Function of the Voltage Response to the Current Pulse

Ivan Radaš *, Nicole Pilat, Daren Gnjatović, Viktor Šunde and Željko Ban

Faculty of Electrical Engineering and Computing, University of Zagreb, 10000 Zagreb, Croatia
* Correspondence: ivan.radas@fer.hr

Abstract: There are several methods for estimating the *SoC* of lithium-ion batteries that use electrochemical battery models or artificial intelligence and intelligent algorithms. These methods have numerous advantages but are complex and computationally intensive. This paper presents a new method for estimating the *SoC* of lithium-ion batteries based on identifying the transfer function of the measured battery voltage response to the charging current pulse. It is assumed that the transfer function of the battery changes with the state of charge. In the learning phase, a reference table of known *SoC*s and associated transfer functions is created. The parameters of these transfer functions form the reference points in hyperspace. In the phase of determining the unknown *SoC* of the battery, the parameters of the measured transfer function form a point in hyperspace that is compared with the reference points of the transfer functions for known *SoC*s. The unknown *SoC* of the battery at the particular measurement time is obtained by finding the two reference points closest to the point of unknown *SoC* using the Euclidean distance and a linear interpolation based on this distance. The method is simple, computationally undemanding, insensitive to measurement noise, and has high accuracy in *SoC* estimation.

Keywords: lithium-ion batteries; estimating the *SoC* of battery; battery's equivalent circuit model; transfer function of battery; Euclidean hyperspace of transfer function parameters

Citation: Radaš, I.; Pilat, N.; Gnjatović, D.; Šunde, V.; Ban, Ž. Estimating the State of Charge of Lithium-Ion Batteries Based on the Transfer Function of the Voltage Response to the Current Pulse. *Energies* **2022**, *15*, 6495. https://doi.org/10.3390/en15186495

Academic Editors: Desmond Gibson, Mojtaba Mirzaeian, Peter Hall and Saule Aidarova

Received: 7 August 2022
Accepted: 1 September 2022
Published: 6 September 2022

1. Introduction

As electricity generation from renewable energy sources has increased, so has the use of energy storage systems. Specific energy, specific power, lifetime, and reliability are among the most important criteria considered when selecting a storage system. There are various electrical energy storage systems, among which the systems of lithium-ion batteries stand out due to their high energy density and acceptable lifetime [1]. The safe, reliable, and efficient operation of batteries requires a battery management system (BMS) that monitors, diagnoses, and keeps the battery in operation. The main parameters monitored and diagnosed by the BMS are state of charge (*SoC*), state of health (SoH), and battery temperature.

There are different definitions of battery capacity and *SoC*. According to [2], *SoC* is defined as the ratio of the charge difference of a fully charged battery C_N and the amount of discharged charge Q_b with respect to the amount of charge of a fully charged battery:

$$SoC = \frac{C_N - Q_b}{C_N} \tag{1}$$

where:

- C_N—charge of the fully charged battery, [Ah],
- Q_b—amount of discharge charge of battery, [Ah].

According to this definition, a full state of charge is reached when the battery current does not change within 2 h at constant charge voltage and temperature. Estimating the *SoC* is not a simple task because the *SoC* depends on the capacity, temperature, and internal resistance of the battery. It is desirable to keep *SoC* of batteries within reasonable and safe limits such as $20\% \leq SoC\% \leq 95\%$ [3].

The *SoC* of a battery cannot be measured directly, but it can be estimated using various methods [4]. Two typical *SoC* evaluation methods are the open circuit voltage (OCV) method and the coulomb method, i.e., the ampere-hour or coulomb counting method. The OCV method estimates *SoC* indirectly by measuring the open-circuit voltage of the battery and using tables with a predetermined *SoC*–OCV relationship. Despite its reliability, this method is not practical in online applications because the battery must be relaxed for a period of time for the open-circuit voltage to reach a steady state. This method is also not suitable for batteries where the open-circuit voltage changes little with changes in the state of charge (flat OCV curve) [5,6]. The coulomb counting method is easy to implement due to its low computational cost, and it is based on numerical integration of the current over time. However, this method requires knowledge of the initial state of charge and is sensitive to the accuracy of the sensor measurements. Additionally, possible sources of error in this method are the reduction of capacity over time and self-discharge [7]. The internal resistance of the battery can also be used to estimate the *SoC*. However, the irregular correlation between the internal resistance and *SoC* is not suitable for the reliable estimation of *SoC* [8].

In addition to the previously mentioned *SoC* evaluation methods, there are also methods that use algorithms based on the battery model. Electrochemical models (EM) are commonly used for *SoC* estimation [9,10]. EM use partial differential equations to model the physics of the battery. To achieve a good balance between computational cost and accuracy, a low-complexity *SoC* prediction method uses a simplified electrochemical model. The battery model can be used to calculate the battery voltage based on the known input current, temperature, and *SoC*. Assuming that the battery model is correct, the calculated voltage would be equal to the measured voltage. Any discrepancy between the battery voltage calculated by the model and the measured voltage can be used to correct the *SoC* at any point during calculation over time. In general, model-based methods such as the Kalman filter (KF), extended Kalman filter (EKF) [11,12], unscented Kalman filter (UKF) [13], H infinite filter (H∞), sliding mode observer [14], and others [15–17] are insensitive to the value of the initial SoC due to the internal closed-loop structure and have high accuracy and excellent stability. However, an accurate battery model is required for accurate *SoC* estimation since it is not possible to correct for modeling errors. Several other variants of the Kalman filter, e.g., sigma-point KF [18], adaptive KF [19], and derivative KF [20], have also been used for *SoC* battery estimation. However, further improvements to the algorithm lead to increased computational costs and implementation difficulties.

With the development of computers and artificial intelligence, intelligent algorithms such as support vector machine (SVM), fuzzy logic, and neural networks (NN) are increasingly used in *SoC* evaluation. Without any information about the internal structure of the battery and the initial *SoC*, these algorithms explore the relationship between the *SoC* and measured variables such as battery voltage, current, and temperature according to the learning data [21–26]. However, the algorithms require a large memory to store the amount of data required for learning, which consequently burdens the entire system and results in long-term procedures and difficulties in implementation.

This paper describes a method for estimating the *SoC* based on the battery model and the relationship between the *SoC* and the dynamic response of the battery, i.e., the battery transfer function. It is assumed that the voltage response function to the current pulse is a nonlinear function of the *SoC*. By determining the transfer function of the voltage response to the current pulse at a particular point of the *SoC*, the parameters of the transfer function that depend on the *SoC* are obtained. The parameters of the transfer function can be considered as the coordinates of the hyperspace point for the corresponding *SoC*. In the learning phase of this method, a map was created to establish a link between the *SoC* and the corresponding transfer functions. The algorithm of the method starts with the online measurement of the voltage response of the battery to the corresponding current pulse and proceeds with the calculation of the parameters of the transfer function. The parameters of the transfer function for the unknown *SoC* form a new point of hyperspace from which the *SoC* of the battery is determined by interpolation from the Euclidean distance to the nearest points. The application of the method is illustrated by the *SoC* assessment of a high-capacity lithium-nickel-manganese-cobalt-oxide ($LiNiCoMnO_2$) battery cell.

The novelty of the method is the estimation of the *SoC* based on the position in hyperspace of the point defined by the parameters of the transfer function and the determination of the parameters of the function by optimization from the time response of the battery voltage to the current pulse. The use of the optimization method to determine the parameters of the transfer function ensures insensitivity to measurement noise and is not very computationally demanding. The method is suitable for determining the *SoC* when the initial *SoC* is not known and has the potential for application to various battery chemistries.

What is special about this method is that it does not require a permanent measurement of the voltage and current at the battery but only the response of the voltage to a current pulse of about 3 s duration. This is especially important when the algorithm is not applied in the battery BMS but in a charging station for light electric vehicle batteries, which have no communication between the vehicle battery BMS and the station.

Methods based on Kalman filters require constant measurement of voltage and current and execution of an algorithm with a specific sampling time, making them suitable for use in BMSs where the BMS computer continuously executes algorithms for voltage monitoring and balancing, battery protection, and state of charge estimation. The algorithm described in this paper does not require the entire algorithm to be executed in real time.

The battery charging station for light electric vehicles can use its own converter to generate a current pulse, record the battery's current and voltage signals, and send the recorded information packet to the monitoring computer in the station. After that, the converter is free to perform the battery charging function. A monitoring computer, which has no time-critical control functions, can perform the battery *SoC* estimation. In this way, the real-time converter controller is not burdened with complex mathematical estimation functions, while the data transmission to the monitoring computer is not time-critical because it is not part of the control loop.

The effectiveness of the proposed method was tested by simulation and experiments. In the second chapter of the paper, the used model of the lithium-ion battery is described; thus, the form of the transfer function is determined. The third chapter describes the principle of the new *SoC* estimation method. The fourth chapter describes the algorithm used in the learning phase, i.e., the formation of the reference base of *SoC*s and associated transfer functions, the laboratory setup used, and the results of the learning process. In the fifth chapter, the results of the determination of the unknown *SoC* using the proposed method are presented, followed by the conclusion.

2. Lithium-Ion Battery

Among several electrical models of the battery, to evaluate the *SoC*, the equivalent circuit model (ECM) is used in this paper. The reasons for using this model are the good balance between accuracy and simplicity of the model. A basic ECM consists of an ideal voltage source, an internal resistance, and an RC circuit that represents the dynamic characteristics of the battery. The reason for the dynamic behavior of batteries is the polarization and diffusion between the battery electrodes.

However, to reliably determine the *SoC* of the battery, it is necessary to extend the basic ECM with another RC circuit [27]. The electrolyte inside the battery separates the battery's electrodes, prevents short circuit, and allows ion flow between the electrodes. The properties of the electrolyte degrade over time, so the electrolyte particles eventually bind to the anode and form a second layer called the solid electrolyte interphase (SEI). As the battery ages, the impact of SEI on battery performance and dynamic behavior becomes more apparent. The basic ECM is extended by an additional RC circuit that models this influence (see Figure 1). The time constant R_1C_1 influences the transfer function of the extended ECM model; however, it was not investigated how this constant, by itself, affects the *SoC*. This influence will be determined in the continuation of the research.

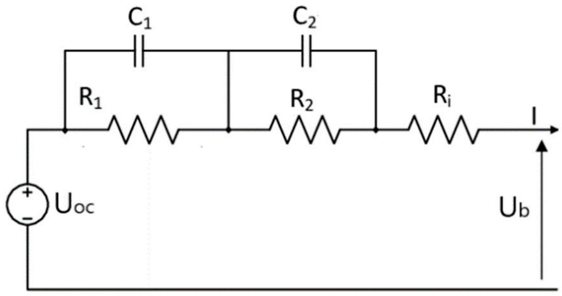

Figure 1. Equivalent Circuit Model of the battery. R_i—internal battery resistance [Ω]; R_1—SEI layer resistance [Ω]; C_1—SEI layer capacity [F]; R_2—battery element resistance [Ω]; C_2—internal battery capacity [F]; *Uoc*—battery open circuit voltage [V].

The voltage changes as a function of the current change at the operating point determined by the *SoC*, and the voltage *Uoc* for the ECM from Figure 1 is determined by a second-order transfer function:

$$G(s) = K\,\frac{b_2 s^2 + b_1 s + b_0}{a_2 s^2 + a_1 s + 1}, \tag{2}$$

where:

- K is the gain of the transfer function.
- $b_i\ \forall\ i = 0, \ldots\ 2$—nominator parameters of the transfer function.
- $a_i\ \forall\ i = 0, \ldots\ 2$—denominator parameters of the transfer function.

The battery voltage in the Laplace domain is determined by the expression:

$$u(s) = U_{OC} + G(s)i(s), \tag{3}$$

where:

- $G(s)$ is the battery transfer function.
- $i(s)$ is the battery current in the Laplace domain [A].
- $u(s)$ is the battery voltage in the Laplace domain [V].

The transfer function (2) contains two zeros and two poles. However, the non-dominant zero and the non-dominant pole have less influence on the response and are very sensitive to measurement noise in the estimation. For this purpose, the estimation requires an equivalent transfer function $G_e(s)$ containing one zero and two poles of the form:

$$G_e(s) = \frac{b_1 s + b_0}{a_2 s^2 + a_1 s + 1}, \tag{4}$$

$$u(s) = U_{OC}(s) + G_e(s)I(s), \tag{5}$$

Estimation determines the parameters of the transfer function that give the response closest to the measured one.

3. Transfer-Function-Based Method for SoC Estimation

The proposed method estimates the unknown *SoC* by comparing the parameters of the transfer function of the battery voltage response to the current pulse determined for this *SoC* with the parameters of the reference transfer functions previously determined at different states of charge in the learning process. The current pulse that excites the voltage response must have a small value to remain in the same operating point. The learning process begins with measurements of the voltage response to the corresponding current pulse, i.e., determining the parameters of transfer functions of the form (4) and (5) for several different and known battery *SoC*s. The following parameters are extracted from the estimated transfer function for each *SoC* and used in the recognition process:

- Open circuit voltage (U_{OC}).
- The gain of the transfer function (b_0).
- The dominant pole of the transfer function.
- Zero of the transfer function ($-b_0/b_1$).

At the end of the learning process, the extracted parameters of the transfer functions are grouped with the corresponding *SoC*s and stored in the corresponding table of reference values. The evaluation of the unknown *SoC* of the battery starts with sending the same current pulse as in the learning process, measuring the voltage response and estimating the transfer function parameters. From the estimated transfer function, the parameters for recognition are determined in the same way as in the learning process. These parameters are then compared to the parameters in the reference table to determine the data set from the table that has the most similar parameter values to the currently determined parameters for the unknown *SoC*. By comparing the estimated parameters with the known parameters from the database, it is possible to uniquely determine the state of charge of the battery.

4. Learning Process

During the learning phase, measurements were taken for nine known *SoC*s, starting with an empty battery and ending with a full battery in 12.5% increments. To verify battery capacity, the battery was first discharged to the cutoff voltage and then charged to the allowable voltage using a constant current/constant voltage method with a charge current equal to 50% of the nominal charge current. The energy delivered was measured using the ampere-counting method. When the charging current dropped to 5% of the nominal charging current, the charging process was complete. This method establishes a relationship between the *SoC* of the battery and the amount of energy stored. The learning process itself began by discharging the battery again and by measuring the voltage response to a small current pulse for each desired point of the *SoC* to establish a table of reference values. For each reference point, the corresponding transfer function and certain parameters to be used for recognition were estimated.

4.1. Learning Algorithm

The learning algorithm is shown in the flowchart in Figure 2. Measurements of the voltage response to a small current pulse were made at the values of stored energy corresponding to the following *SoC* (%) values: [0, 12.5, 25.0, 37.5, 50.0, 62.5, 75.0, 87.5, 100].

The measurement of stored energy to determine the reference point of charge was performed using the ampere-counting method.

At each of the reference points of the *SoC*, the voltage response to a small current pulse was recorded. The recorded current and voltage signals were stored with the corresponding *SoC* of the battery. The procedure for estimating the transfer function parameters for each *SoC* was performed by optimizing the parameters of the model determined by Equations (4) and (5).The parameters were optimized using the Nelder–Mead simplex method implemented in MATLAB according to the minimum of the *ISE* criterion defined by the equation:

$$ISE = \int_0^T [u(t) - u_m(t)]^2 dt \tag{6}$$

where:

- $u(t)$ is the measured battery voltage response signal to the current pulse.
- $u_m(t)$ is the voltage response signal of the battery model to the measured current pulse signal.
- T is the duration of the simulation.

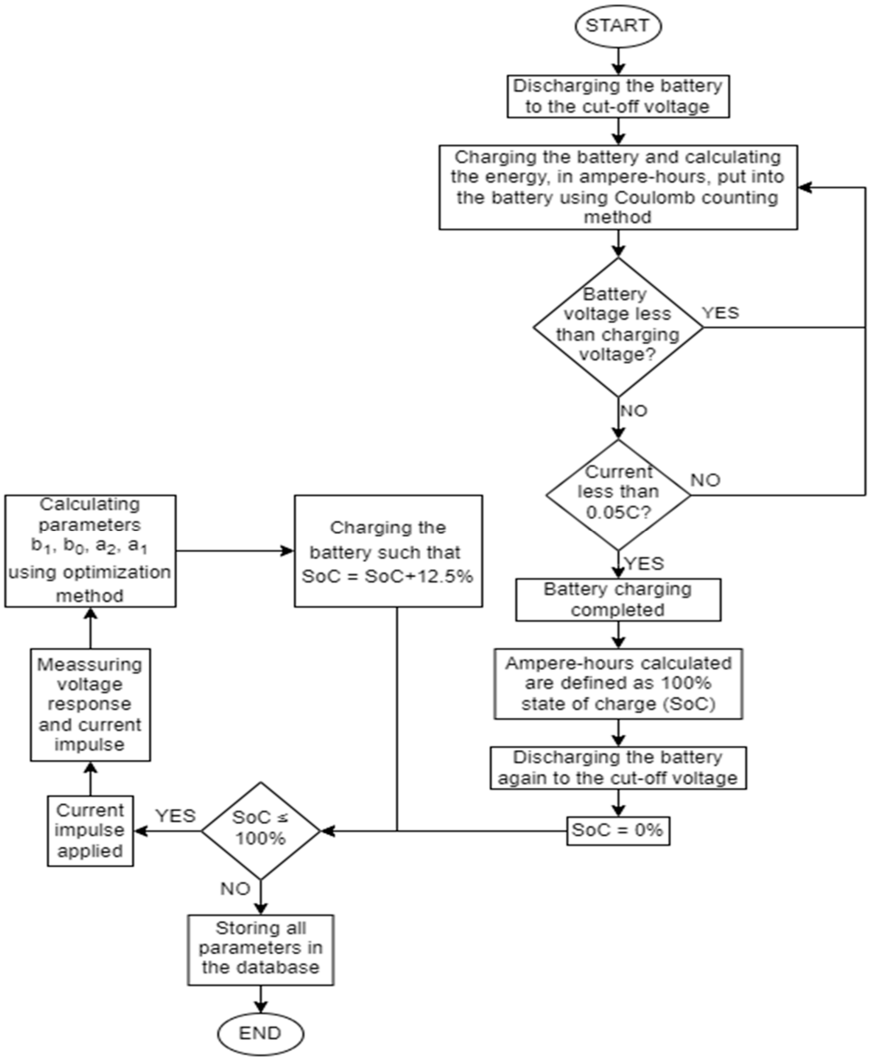

Figure 2. Flowchart of the learning process.

In the estimation, the calculation of the criteria was performed during the entire time of the signal measurement, i.e., until the battery voltage stabilizes after the current pulse drops to zero.

For this purpose, the MATLAB/Simulink battery voltage model is defined according to Equations (4) and (5), as shown in Figure 3.

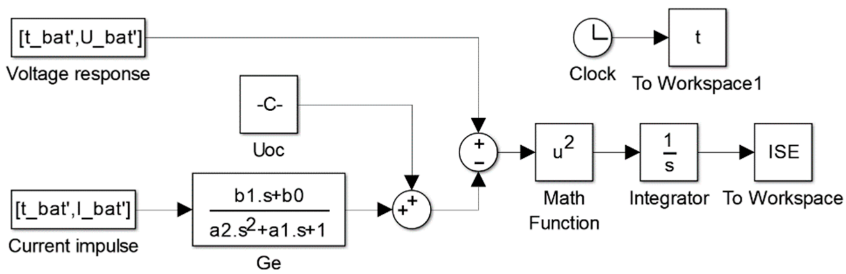

Figure 3. Matlab/Simulink model of the battery voltage for calculating the optimization criterion.

The transfer function of the dynamic part of the model in block Ge is described by Equation (4).

The parameter in block *Uoc* was determined before optimization as the average of the voltage signal before exposure to the current pulse, while the transfer function parameters were determined by optimization with the simplex method using the MATLAB *fminsearch* function from the optimization toolbox.

The vector of optimization parameters is defined by the expression:

$$\boldsymbol{x} = [\, b_1\; b_0\; a_2\; a_1] \tag{7}$$

The estimated transfer function is not limited to the aperiodic response of the voltage to the current pulse but also includes transient responses with overshoot.

From the estimated parameters of the transfer function G_e, the parameters of the reference table are determined for each *SoC*:

$$\boldsymbol{x_R} = [Uoc\;\; K\; z\; p] \tag{8}$$

$$z = -\frac{b_0}{b_1} \tag{9}$$

$$K = b_0 \tag{10}$$

The dominant pole, i.e., the root of the denominator of the transfer function, is defined as the root of the denominator whose real part is closest to the origin. This was performed with MATLAB functions:

$$G_e = tf([b_1\; b_0], [a_2\; a_1\; 1]) \tag{11}$$

$$p = pole(G_e) \tag{12}$$

$$i = find(abs(real(p)) = min(abs(real(p)))) \tag{13}$$

$$p = real(p(i)) \tag{14}$$

For each *SoC* measured in this way, a reference vector $\boldsymbol{x_R}$ is determined, which can be represented by a point in four-dimensional Cartesian hyperspace.

To increase the accuracy of learning, it is possible to perform multiple measurements and estimations of transfer functions for the same *SoC* to obtain more associated vectors, i.e., points of the hyperspace for one *SoC*. In this case, the points form a cloud for the corresponding *SoC*, and the reference point to which the reference vector belongs is calculated as the centroid of the cloud points for each *SoC*.

The table of *SoC*s and associated vectors $\boldsymbol{x_R}$ defines a piecewise linear function of the dependence of the *SoC* on the vector $\boldsymbol{x_R}$. Based on this, the determination of the unknown *SoC* can be carried out from the estimated values of the associated vector $\boldsymbol{x_R}$ by finding two points with the smallest Euclidean distance from the point with the unknown *SoC* and determining the *SoC* by linear interpolation.

4.2. Experimental Setup for Learning

The experimental part of the research in the learning phase consisted of several charging and discharging cycles of the battery to determine the voltage profile, battery capacity, and the effects of charging power on battery temperature. The following equipment was used for the experiment:

- Battery—SAMSUNG ICR 18,650—26 J M
- Current sensor—HY 5-P,48,275, JP2
- Current source—Magna—Power electronics, XR 50-40, 2 kW
- Current pulse source—Iskra Power Supply (IPS), MA 4171, 1 A, 25 V
- Laboratory Power Supply (LPS), PS—24,030, 0–40 V, 0.01–3 A
- Electronic load—Hewlett Packard—6050a
- Microcomputer for measurement and control—*dSPACE—MicroLabBox*
- MATLAB/Simulink package on the PC computer

Battery specifications are given in Table 1.

Table 1. Battery specifications.

Item	Specification
Nominal Capacity	2600 mAh (0.2 C, 2.75 V discharge)
Charging Voltage	4.2 ± 0.05 V
Nominal Voltage	3.63 V
Standard Charging Current	1300 mA
Charging Time	3 h
Max. Charge Current	2600 mA (ambient temperature 25 °C)
Max. Discharge Current	5200 mA (ambient temperature 25 °C)
Discharge Cut-off Voltage	2.75 V
Cathode	$LiNi_{1/3}Co_{1/3}Mn_{1/3}O_2$
Anode	Graphite

The equivalent electrical diagram of the laboratory setup is shown in Figure 4, while the actual appearance of the laboratory setup is shown in Figure 5.

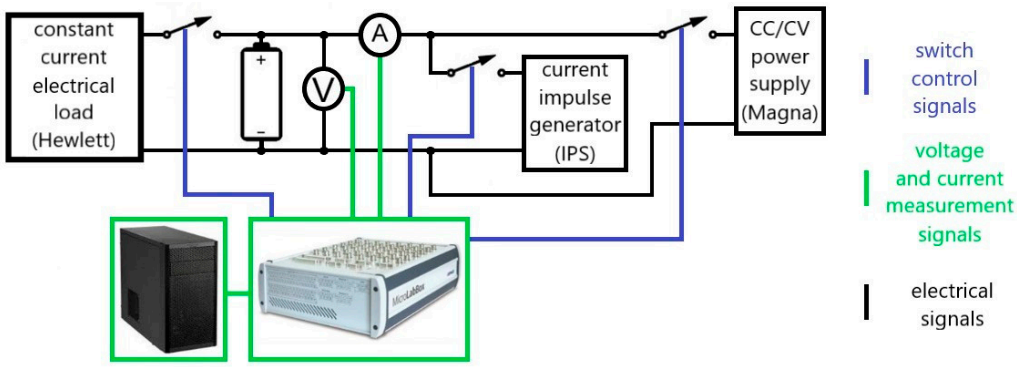

Figure 4. Electrical scheme of the experimental setup.

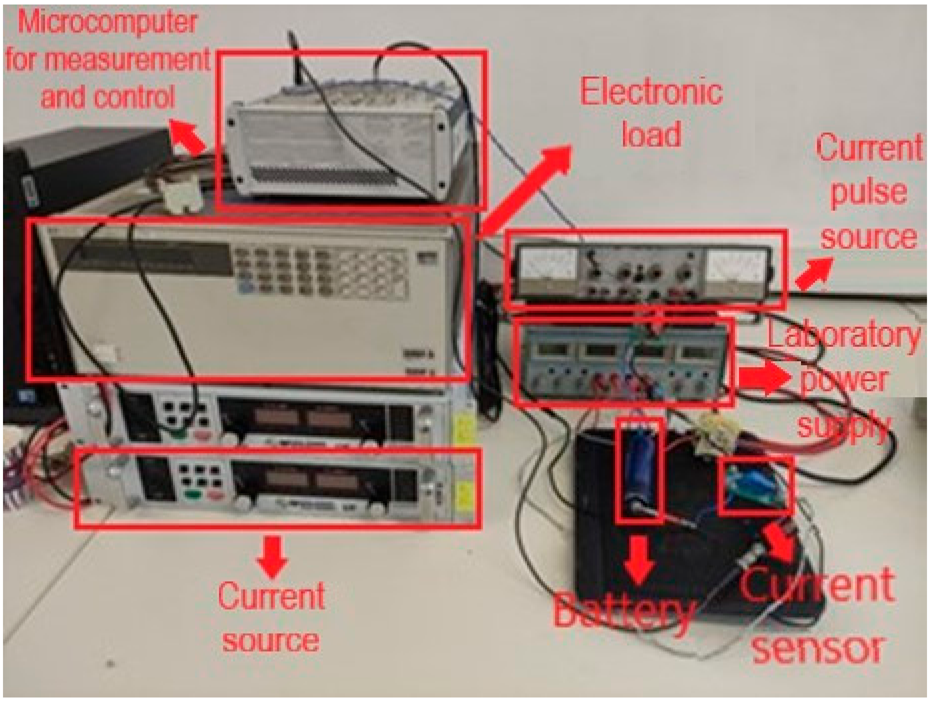

Figure 5. Experimental setup.

A MATLAB script and real-time toolbox were used to control the dSpace microcomputer to synchronize controllable sources and measurements. Measurements and recording of measurement results were performed using dSPACE MicroLabBox. The sampling time was set to 100 µs to record the dynamic voltage response. All further data processing and parameter estimation were performed offline from the measured data in MATLAB/Simulink using the optimization toolbox, as described in the previous chapter.

4.3. Experimental Results of the Learning Phase

In the learning process, the battery for a given *SoC* is excited by a current pulse, as shown in Figure 6.

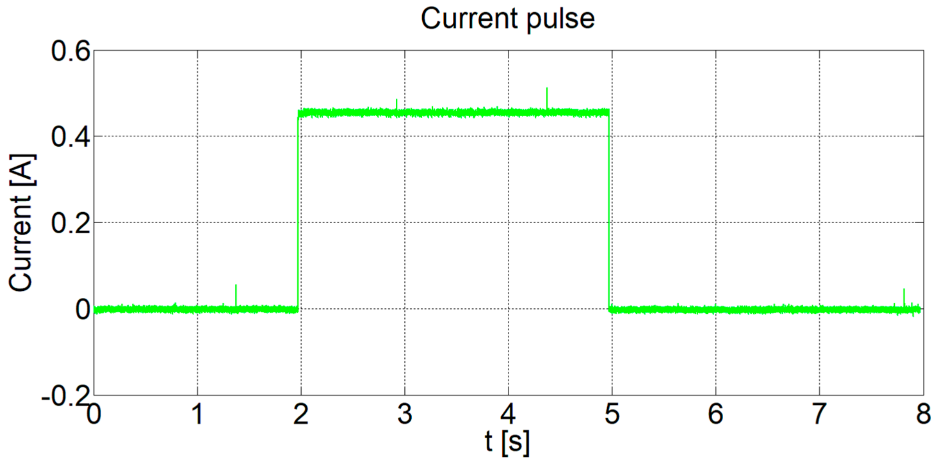

Figure 6. Current pulse.

Nine *SoC* reference points were selected, evenly distributed in the range from 0 to 100%. Experiments have shown that nine points provide estimation accuracy with an error below 5%. For each state of charge (%) (0, 12.5, 25, 37.5, 50, 62.5, 75, 87.5, 100), multiple voltage responses are measured for identical current pulses. The transfer function parameters are calculated from each voltage response through an optimization process to obtain parameters for which the error in voltage estimation is minimal according to the ISE criterion.

Figure 7 shows the measured voltage response to the current pulse and the Simulink model voltage with estimated parameters for the reference point *SoC* = 50%. The difference between the signals is caused by noise. When this learning process is completed for all reference points, i.e., *SoC*s, the vector of transfer function coefficients x_R is stored in the reference table with the corresponding *SoC*. This completes the learning phase. The matrix of learned values for the battery SAMSUNG ICR 18650–26J M is shown in Table 2.

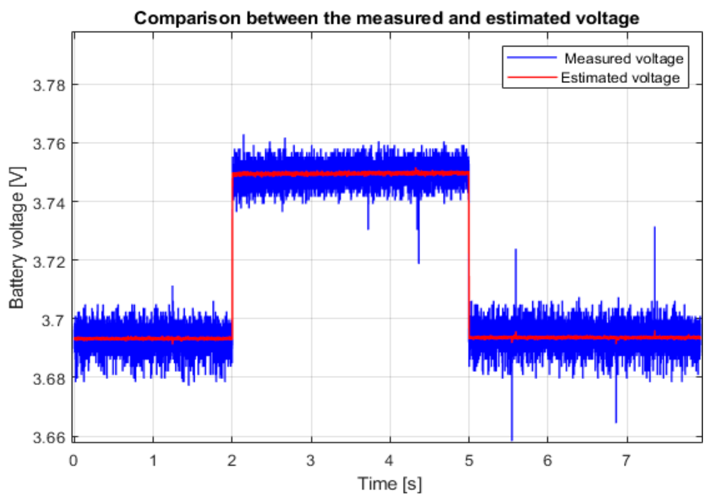

Figure 7. Measured and model of calculated voltage according to estimated parameters.

Table 2. Reference table of learned values.

SoC [%]	U_{OC} [V]	*K*	*z*	*p*
0	2.7353	0.4236	−0.1220	−0.0332
12.5	3.4466	0.1090	−0.0412	−0.0392
25	3.5750	0.1090	−0.0412	−0.0392
37.5	3.6795	0.1201	−0.0584	−0.0500
50	3.7980	0.1251	−0.0664	−0.0530
62.5	3.9068	0.1206	−0.0647	−0.0512
75	4.0276	0.1240	−0.0469	−0.0381
87.5	4.1228	0.1005	−0.0510	−0.0519
100	4.1697	0.1587	−0.0544	−0.0347

5. Estimation of the Unknown SoC

The process of *SoC* estimation consists of three phases: (i) measurements of the voltage response to the current pulse at the studied *SoC*, (ii) estimation of the vector $\boldsymbol{x} = [U_{OC}\ K\ z\ p]$ in the same way as in the learning processes, and (iii) localization of the point in hyperspace determined by the test vector. The process of estimating the unknown *SoC* is represented by the flowchart in the Figure 8.

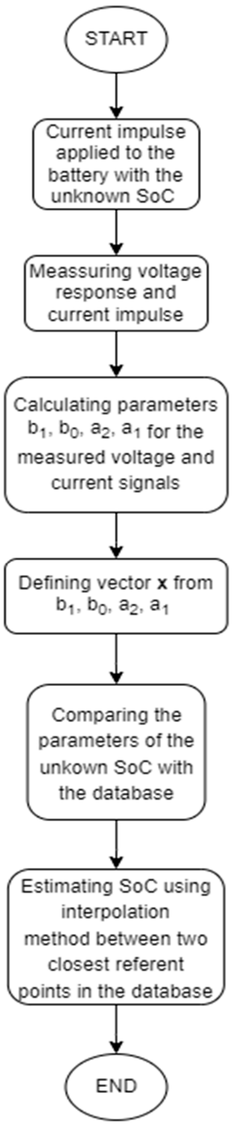

Figure 8. Flowchart for estimating unknown *SoC*.

The evaluation of the *SoC* starts with the measurement of the voltage response of the battery to the current pulse with similar characteristics as in the learning phase.

The voltage response is used to calculate the U_{OC} and the coefficients of the transfer function of the battery at the tested state of charge. The test vector $\boldsymbol{x_T}$ is determined from the estimated parameters. The test vector $\boldsymbol{x_T}$ determines a single point in hyperspace.

By determining its distance to the nearest reference points from the reference table, the corresponding *SoC* is estimated by interpolation.

The estimation of the corresponding *SoC* for the point determined by the vector $\boldsymbol{x_T}$ is performed in two steps. First, the value of the parameter U_{OC} is used to determine whether the vector belongs to one of the three ranges of *SoC*: [$SoC < 25\%$, $25\% \leq SoC \leq 75\%$, $SoC > 75\%$].

In this way, the U_{OC} has the greatest weight in determining the range. Then, the two points of the reference table closest to the point determined by the vector $\boldsymbol{x_T}$ for the unknown *SoC* within the specified range are found.

For the localization of the test vector in hyperspace, the distance between two points is calculated based on the Euclidean norm according to the following equation:

$$d = \sqrt{\left(K_{test} - K_{ref}\right)^2 + \left(p_{test} - p_{ref}\right)^2 + \left(U_{OC,\,test} - U_{OC,ref}\right)^2 + \left(z_{test} - z_{ref}\right)^2} \quad (15)$$

where:

- K is the system gain for measured and reference *SoC*.
- p is the dominant pole of transfer function for measured and reference *SoC*.
- U_{OC} is the open-circuit battery voltage before current impulse for the measured and the reference *SoC*.
- z is the zero of the transfer function for the measured and reference *SoC*.

The index *test* defines the membership of the parameter to the $\boldsymbol{x_T}$ vector, and the *ref* index defines the parameter membership to the $\boldsymbol{x_R}$ vector of the reference table.

In estimating the unknown *SoC*, a linear change in the *SoC* between two reference points is assumed, proportional to the distance between them.

Using the Euclidean norm, the two distances d_1 and d_2 corresponding to the two closest points of the reference table within the defined area of the *SoC* are determined. The distance d_1 is the distance to the point with the lower *SoC*, while d_2 is the distance to the point with the higher *SoC*.

The unknown *SoC* represented by the vector $\boldsymbol{x_T}$ is determined by interpolation according to the equation:

$$SoC_{est} = SoC_{low} + \frac{SoC_{high} - SoC_{low}}{d_1 + d_2} * d_1\,, \quad (16)$$

where:

- d_1 is the distance from the point of the unknown *SoC* determined by the vector $\boldsymbol{x_T}$ to the point SoC_{low}.
- d_2 is the distance from the point of unknown *SoC* determined by the vector $\boldsymbol{x_T}$ to the point SoC_{high}.
- SoC_{low}, SoC_{high} are the two points closest to the point of the unknown *SoC* determined by the $\boldsymbol{x_T}$ vector.

5.1. Experimental Results of the SoC Estimation

In order to verify the success of the estimation algorithm, it is necessary to run it at points other than the reference points, since the error at the reference points is negligible. Since the state-of-charge estimation algorithm determines the closest *SoC* reference points to the *SoC* being estimated and performs linear interpolation based on the distance to the reference points, the largest error is expected to occur at the *SoC* farthest from the reference points. The reference points define eight intermediate intervals, and the *SoC*s farthest from the reference points are in the middle of the intervals. Therefore, to examine the worst-case estimation, eight test points located at the halves of the intervals defined by the reference points were selected. Thus, the test procedure for the *SoC* (%) assessment algorithm includes eight points (6.25, 18.75, 31.25, 43.75, 56.25, 68.75, 81.25, 93.75). The evaluation results for eight test points are shown in Table 3.

Table 3. Results of *SoC* estimates.

True *SoC* [%]	Lower Bound for *SoC* [%]	Upper Bound for *SoC* [%]	Estimated *SoC* [%]	Relative Error [%]
6.25	0.00	12.50	5.61	9.57
18.75	12.50	25.00	18.46	1.58
31.25	25.00	37.50	31.42	0.55
43.75	37.50	50.00	43.72	0.08
56.25	50.00	62.50	56.21	0.07
68.75	62.50	75.00	69.03	0.41
81.25	75.00	87.50	81.06	0.23
93.75	87.50	100.00	93.49	0.28

5.2. Analysis of the Results of the SoC Estimation

The first column of Table 3 shows the actual *SoC* obtained by applying the coulomb counting method, in percent. The second and third columns show between which two reference points the unknown *SoC* is located. The fourth column shows the estimated *SoC* value based on Equation (16). The last column shows the relative estimation error, which is calculated as the ratio of the difference between the actual *SoC* value and the estimated *SoC* value relative to the reference *SoC* value. From Table 3, it can be seen that each test point is accurately located, and the estimated *SoC* value is very close to the actual value. The relative error is less than 2% in most cases. The only exception is 6.25%, where the relative error is almost 10%. Generally, at low states of charge, the nonlinearity of the battery is more pronounced, so the linear interpolation increases the estimation error. This will always be the case because with more pronounced nonlinearity, the interpolation method deviates more and more from the exact solution. Nonetheless, we can be certain that the battery is at low states of charge, which can be used to protect a battery from over-discharging. In this case, the estimated *SoC* of 5.61% is below the true *SoC* value of 6.25%.

6. Conclusions

The problem of estimating the *SoC* of lithium-ion batteries is complex, and solutions vary depending on the accuracy and speed requirements of the estimation and the resources used to implement the algorithm. In this paper, we propose an estimation of the *SoC* that does not require knowledge of the initial *SoC* and charging history and is based on the analysis of the estimated coefficients of the transfer function measured at the unknown *SoC*. The transfer function coefficients are estimated by an optimization procedure, i.e., by minimizing the error between the measured signal and the battery model response. The method is accurate in estimating the coefficients but requires high accuracy of the measured data to capture the full dynamics of the battery voltage response. The learning algorithm for determining the matrix of reference values used to estimate the *SoC* is presented. The learning algorithm requires a certain number of measurements to define the matrix of reference values, but once defined, it is usable for all battery cells of the same chemistry and nominal voltage. It is possible to redefine the reference data for a different nominal voltage by changing the existing values. The detection is performed in three phases: (i) measurement of the voltage response to a standardized current pulse, (ii) estimation of the value of the coefficients of the measured transfer function at the unknown *SoC*, and (iii) localization of the point defined by the estimated coefficients of the obtained transfer function according to the measured data in hyperspace and calculation of the unknown *SoC* by interpolation relative to two nearest reference points.

The method is designed for real-time operation where time is not an issue, as the estimation takes an average of 80 s to compute the coefficients of the transfer function and calculate the *SoC*. Computation was performed on a computer with an Intel(R) Core(TM) i5-8300H processor CPU @ 2.30 GHz and 8 GB of RAM (7.88 GB usable). Using a reference table with nine learned points, an error of less than 2% was obtained, except in the *SoC* range between 0 and 12.5%, where the error is significantly higher. Initial tests show that by increasing the number of reference points, especially in the higher error range, the *SoC* estimation error can be reduced to less than 1% of the *SoC* over the entire range.

Author Contributions: Conceptualization, V.Š. and Ž.B.; Data curation, I.R.; Investigation, I.R., N.P., D.G., Ž.B. and V.Š.; Resources, Ž.B.; Software, I.R.; Supervision, V.Š. and Ž.B.; Validation, V.Š. and Ž.B.; Writing—original draft, I.R.; Writing—review & editing, I.R., V.Š. and Ž.B. All authors have read and agreed to the published version of the manuscript.

Funding: All the costs of publishing of this paper are co-financed by the project" KK.01.2.1.01.0134—Mareton—Development of a new generation of industrial modular, redundant, multi-output continuous power supply systems with direct and alternating voltages" co-funded under the Competitiveness and Cohesion Operational Program from the European Regional Development Fund.

Institutional Review Board Statement: Not applicable.

Informed Consent Statement: Not applicable.

Conflicts of Interest: The authors declare no conflict of interest.

References

1. Tie, S.F.; Tan, C.W. A review of energy sources and energy management system in electric vehicles. *Renew. Sustain. Energy Rev.* **2013**, *20*, 82–102. [CrossRef]
2. Sauer, D.U.; Bopp, G.; Jossen, A.; Garche, J.; Rothert, M.; Wollny, M. State of charge—What do we really speak about? In Proceedings of the 21st International Telecommunications Energy Conference, Copenhagen, Denmark, 9 June 1999.
3. Chiasson, J.; Vairamohan, B. Estimating the state of charge of a battery. In Proceedings of the 2003 American Control Conference, Transactions on Control Systems Technology, Denver, CO, USA, 4–6 June 2003; Volume 13, pp. 465–470.
4. Plett, L. *Battery Management System Requirements*; University of Colorado Lecture: Boulder, CO, USA, 2015.
5. Piller, S.; Perrin, M.; Jossen, A. Methods for state-of-charge determination and their applications. *J. Power Sources* **2001**, *96*, 113–120. [CrossRef]
6. Pop, V.; Bergveld, H.J.; Notten, P.H.L.; Regtien, P.P.L. State-of-the-art of battery state-of-charge determination. *Meas. Sci. Technol.* **2005**, *16*, R93–R110. [CrossRef]
7. Ng, K.S.; Moo, C.-S.; Chen, Y.-P.; Hsieh, Y.-C. Enhanced coulomb counting method for estimating state-of-charge and state-of-health of lithium-ion batteries. *Appl. Energy* **2009**, *86*, 1506–1511. [CrossRef]
8. Waag, W.; Käbitz, S.; Sauer, D.U. Experimental investigation of the lithium-ion battery impedance characteristic at various conditions and aging states and its influence on the application. *Appl. Energy* **2013**, *102*, 885–897. [CrossRef]
9. Wu, L.; Liu, K.; Pang, H.; Jin, J. Online SOC Estimation Based on Simplified Electrochemical Model for Lithium-Ion Batteries Considering Current Bias. *Energies* **2021**, *14*, 5265. [CrossRef]
10. Wu, L.; Pang, H.; Geng, Y.; Liu, X.; Liu, J.; Liu, K. Low-complexity state of charge and anode potential prediction for lithium-ion batteries using a simplified electrochemical model-based observer under variable load condition. *Int. J. Energy Res.* **2022**, *46*, 11834–11848. [CrossRef]
11. Plett, G.L. Extended Kalman filtering for battery management systems of LiPB-based HEV battery packs: Part 3. State and parameter estimation. *J. Power Sources* **2004**, *134*, 277–292. [CrossRef]
12. Plett, L. Extended kalman filtering for battery management systems of lipb-based hev battery packs: Part 1. Background. *J. Power Sources* **2004**, *134*, 252–261. [CrossRef]
13. Santhanagopalan, S.; White, R.E. State of charge estimation using an unscented filter for high power lithium ion cells. *Int. J. Energy Res.* **2009**, *34*, 152–163. [CrossRef]
14. Kim, I.-S. The novel state of charge estimation method for lithium battery using sliding mode observer. *J. Power Sources* **2006**, *163*, 584–590. [CrossRef]
15. Smith, K.A.; Rahn, C.D.; Wang, C.-Y. Model-based electrochemical estimation of Lithium-ion batteries. In Proceedings of the IEEE International Conference on Control Applications, San Antonio, TX, USA, 3–5 September 2008; pp. 714–719.
16. Verbrugge, M.; Tate, E. Adaptive state of charge algorithm for nickel metal hydride batteries including hysteresis phenomena. *J. Power Sources* **2004**, *126*, 236–249. [CrossRef]
17. Hu, Y.; Yurkovich, S. Battery cell state-of-charge estimation using linear parameter varying system techniques. *J. Power Sources* **2012**, *198*, 338–350. [CrossRef]
18. Plett, G.L. Sigma-point Kalman filtering for battery management systems of LiPB-based HEV battery packs: Part 2: Simultaneous state and parameter estimation. *J. Power Sources* **2006**, *161*, 1369–1384. [CrossRef]

19. Sepasi, S.; Ghorbani, R.; Liaw, B.Y. A novel on-board state-of-charge estimation method for aged Li-ion batteries based on model adaptive extended Kalman filter. *J. Power Sources* **2014**, *245*, 337–344. [CrossRef]
20. Antaloae, C.; Marco, J.; Assadian, F. A Novel Method for the Parameterization of a Li-Ion Cell Model for EV/HEV Control Applications. *IEEE Trans. Veh. Technol.* **2012**, *61*, 3881–3892. [CrossRef]
21. Li, S.G.; Sharkh, S.M.; Walsh, F.C.; Zhang, C.N. Energy and Battery Management of a Plug-In Series Hybrid Electric Vehicle Using Fuzzy Logic. *IEEE Trans. Veh. Technol.* **2011**, *60*, 3571–3585. [CrossRef]
22. Chen, J.; Ouyang, Q.; Xu, C.; Su, H. Neural Network-Based State of Charge Observer Design for Lithium-Ion Batteries. *IEEE Trans. Control Syst. Technol.* **2017**, *26*, 313–320. [CrossRef]
23. Chemali, E.; Kollmeyer, P.J.; Preindl, M.; Ahmed, R.; Emadi, A.; Kollmeyer, P. Long Short-Term Memory Networks for Accurate State-of-Charge Estimation of Li-ion Batteries. *IEEE Trans. Ind. Electron.* **2018**, *65*, 6730–6739. [CrossRef]
24. Sahinoglu, G.O.; Pajovic, M.; Sahinoglu, Z.; Wang, Y.; Orlik, P.V.; Wada, T. Battery State-of-Charge Estimation Based on Regular/Recurrent Gaussian Process Regression. *IEEE Trans. Ind. Electron.* **2017**, *65*, 4311–4321. [CrossRef]
25. Chaoui, H.; Ibe-Ekeocha, C.C. State of Charge and State of Health Estimation for Lithium Batteries Using Recurrent Neural Networks. *IEEE Trans. Veh. Technol.* **2017**, *66*, 8773–8783. [CrossRef]
26. Hu, J.; Lin, H.; Li, X.; Jiang, C.; Qiu, X.; Li, W. State-of-charge estimation for battery management system using optimized support vector machine for regression. *J. Power Sources* **2014**, *269*, 682–693. [CrossRef]
27. El-Sehiemy, R.; Hamida, M.A.; Elattar, E.; Shaheen, A.; Ginidi, A. Nonlinear Dynamic Model for Parameter Estimation of Li-Ion Batteries Using Supply–Demand Algorithm. *Energies* **2022**, *15*, 4556. [CrossRef]